Preprints of the 19th World Congress
The International Federation of Automatic Control
Cape Town, South Africa. August 24-29, 2014

Modelling and Control of a Suspended-Span Bridge Section

Xiaowei Zhao * **David J N Limebeer** **
J Michael R Graham ***

* *School of Engineering,*
University of Warwick, Coventry CV4 7AL, U.K.
(e-mail: xiaowei.zhao@warwick.ac.uk)
** *Department of Engineering Science,*
University of Oxford, Oxford OX1 3PJ, U.K.
(e-mail: david.limebeer@eng.ox.ac.uk)
*** *Department of Aeronautical Engineering,*
Imperial College London, London SW7 2AZ, U.K.
(e-mail: m.graham@imperial.ac.uk)

Abstract: We study the modelling and flutter suppression of a suspended-span bridge section using aerodynamic control means. The aerodynamic actuators are controllable leading- and trailing-edge flaps fitted to both edges of the bridge deck. The modelling is based on thin aerofoil theory which describes the bridge deck - air stream interactions. The model also consider the mass and inertia effects of the flaps. Passive mechanical controllers are proposed that sense the vertical velocity of the leading- and trailing-edge flap pivots and use these signals to produce control torques and adjust the flap angles accordingly. The control system is insensitive to the wind direction in the case of identical leading- and trailing-edge mechanical controllers. The Akashi-Kaikyo bridge is used as a working example for the numerical simulation evaluation of the control system performance.

1. INTRODUCTION

Long-span bridges can be susceptible to wind excitation due to their low structural damping and inherent flexibility in combination with aerodynamically inappropriate bridge deck profiles. The Tacoma Narrows bridge disaster was caused by wind induced oscillations called flutter Billah and Scanlan [1991]. In order to satisfy the requirement for increasingly long bridge spans a combination of cautionary steps are taken against possible flutter instabilities including: modifications to the deck's aerodynamic design, modifications to the suspension system to adjust beneficially the bridge's critical structural mode shapes and modal frequencies and the introduction of controllable aerodynamic surfaces e.g. flaps Astiz [1998]. In the case of very long-span bridges, purely structural solutions lead to impractically deep deck sections with high associated weights and/or costs. In this paper we describe research into the suppression of wind-induced oscillations in long-span suspension bridges using aerodynamic (feedback) control that exploits flaps fitted to both the trailing and leading edges of the bridge deck; see Fig. 1. The control purpose is to increase the critical flutter speed. If successful, this technology will help permit the construction of bridges with significantly longer spans.

The literature in this area can be classified to be four broad categories. Active controllers, such as those based on linear optimal control and $\mathcal{H}_\infty$ Hansen and Thoft-Christensen [2001], face severe reliability questions, because they are relatively complicated and will require a power supply and probably also a computer system. Bad

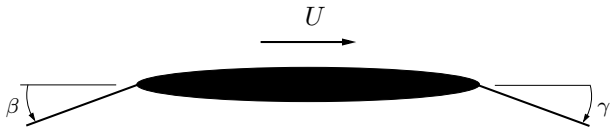

Fig. 1. Cross section of a long-span suspension bridge fitted with controllable leading- and trailing-flaps. U is the wind speeds; β and γ are the leading- and trailing-edge flap angles respectively.

weather situations may well result simultaneously in high winds and power supply failures. Adaptive controllers, such as variable gain output feedback controllers Wilde and Fujino [1996], face the same set of difficulties. Fixed-phase controllers, such as those described in del Arco and Aparicio [1999], are not physically realizable. Realizable systems that introduce frequency-dependent phase compensation may operate satisfactorily, but this has not thus far been established. Passive pure-gain controllers Omenzetter et al. [2000a,b] are in principle easy to implement, but these systems forego the advantages that might accrue from phase compensation such as robustness.

We have spent a lot of efforts to solve the above shortcomings using the mechanical controller concept, which has been successfully used in motorcycle steering Evangelou et al. [2007]. In Graham et al. [2011a] and Graham et al. [2011b] we developed a simple sectional model with controllable leading- and trailing-edge flaps, which represents both the structural and aerodynamic properties of a long-span suspension bridge. This model ignores the mass and moments of inertia of the flaps, and uses the

flap angles as control inputs. The key finding is that the critical wind speeds for flutter and torsional divergence of the sectional model can be greatly increased, with good stability robustness, through passive feedback control. We used the Akashi-Kaikyo Bridge as our working example and show that the critical wind speed can be increased to 80 m/s (from 52 m/s) with good robust stability margins. The use of static winglets has already been suggested in the literature del Arco and Aparicio [1999]. The results presented in del Arco and Aparicio [1999] are based on the unrealistic assumption that the winglets and main deck are aerodynamically independent. Our results in Graham et al. [2011a] and Graham et al. [2011b], which take account of this aerodynamic interaction, show that static winglets are ineffective in increasing the critical wind speed relating to torsional divergence instability. For that reason alternative approaches to this problem are still required.

In Limebeer et al. [2011] we used a sectional model with a controllable trailing-edge flap to demonstrate the use of feedback for buffet suppression. In this study we use the von Kármán turbulence spectrum to generate vertical wind gust turbulence that acts on the bridge deck causing buffet response. The system used in Limebeer et al. [2011] controls the torque acting on the trailing-edge flap and is responsive to deck movements. We show that a control system realized by a mechanical network can substantially improve the critical flutter speed, while simultaneously suppressing the buffeting response of the bridge structure.

All the results obtained so far depend on the wind direction. In the present paper we develop an extended model that includes leading- and trailing-edge flaps with their inertial effects. On the basis of this model we conduct controller design studies for flutter suppression that include identical mechanical controllers for each flap. We show that this symmetrization of the control system makes it insensitive to wind direction.

The structural and aerodynamic components of the model used in the paper are presented in Section 2. A mechanical network for flaps feedback control is described in Section 3. The main results are given in Section 4, where the properties of the Akashi-Kaikyo bridge and flutter controller optimization problems are described.

2. DYNAMIC MODEL

In this section we derive the structural model and aerodynamic model of the suspended-span bridge section to be used in the paper.

2.1 Structural Model

We will now derive the structural model for the suspended-span bridge section with controllable flaps, whose kinematics are illustrated in Fig. 2. The deck's pitch angle α, heave h and the leading- and trailing-edge flap angles β and γ are the generalized coordinates. By using the standard laws of classical mechanics, one obtains the following equations of motion:

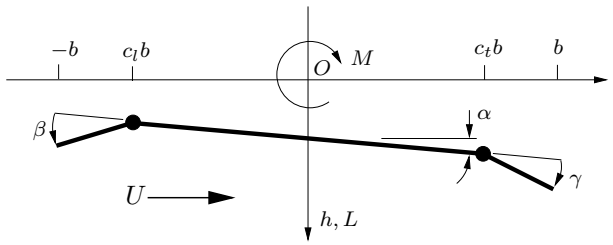

Fig. 2. Kinematic model of the bridge deck. O is the origin of the inertial axis system. The wind velocity U is positive to the right, the lift force L and heave h are positive downwards. The pitch angle α, the trailing-edge flap angles γ and the moment M are positive clockwise, while the leading-edge flap angle β is positive anti-clockwise. The deck (including the flaps) has a width of $2b$ while the leading- and trailing-edge flaps have width of $(1 + c_l)b$ and $(1 - c_t)b$ respectively where $c_l < 0$.

$$m\ddot{h} + S_\alpha\ddot{\alpha} + S_\beta\ddot{\beta} + S_\gamma\ddot{\gamma} = L - K_h h, \tag{1}$$

$$S_\alpha\ddot{h} + I_\alpha\ddot{\alpha} - (I_\beta - bc_l S_\beta)\,\ddot{\beta} + (I_\gamma + bc_t S_\gamma)\,\ddot{\gamma} = M - K_\alpha\alpha, \tag{2}$$

$$S_\beta\ddot{h} - (I_\beta - bc_l S_\beta)\,\ddot{\alpha} + I_\beta\ddot{\beta} = M^\beta - K_\beta\beta, \tag{3}$$

$$S_\gamma\ddot{h} + (I_\gamma + bc_t S_\gamma)\,\ddot{\alpha} + I_\gamma\ddot{\gamma} = M^\gamma - K_\gamma\gamma, \tag{4}$$

in which L and M are the aerodynamic lift force and the aerodynamic moment acting on the bridge deck. The aerodynamic moments M^β and M^γ act on the leading- and trailing-edge flap assemblies. The other parameters in these equations include the leading- and trailing-edge flap angles β and γ (as defined in Fig. 2); m is the mass per unit length of the whole deck assembly; K_h and K_α are the per unit length heave and torsional stiffnesses of the whole assembly; K_β and K_γ are per unit length leading- and trailing-edge torsional stiffnesses of the flaps around their pivot points $c_l b$ (note $c_l < 0$) and $c_t b$; the quantities S_α, S_β and S_γ (I_α, I_β and I_γ) are the per unit length static moments (moments of inertia) of the whole assembly about the points O, $c_l b$ and $c_t b$ respectively; J_d, J_β and J_γ are the per unit length torsional moments of inertia of the bridge deck, and the leading- and trailing-edge flaps, about the points O, $c_l b$ and $c_t b$ respectively. The mass per unit length of the whole assembly is given by $m = m_d + m_\beta + m_\gamma$, where m_d, m_β and m_γ are mass of the bridge deck, and the leading- and trailing-edge flaps.

We suppose also that $K_h = m\omega_h^2$, $K_\alpha = I_\alpha\omega_\alpha^2$, $K_\beta = I_\beta\omega_\beta^2$ and $K_\gamma = I_\gamma\omega_\gamma^2$, in which ω_h, ω_α, ω_β and ω_γ are the undamped natural frequencies of the heave mode, the pitch mode, and the leading- and trailing-edge flap modes. The static moments and moments of inertia are given by:

$$\begin{aligned}
S_\alpha &= bm_d(c_t + c_l)/2 - bm_\beta(1 - c_l)/2 + bm_\gamma(1 + c_t)/2,\\
S_\beta &= bm_\beta(1 + c_l)/2,\\
S_\gamma &= bm_\gamma(1 - c_t)/2,\\
I_\alpha &= J_d + J_\beta + J_\gamma + m_d\left(b(c_t + c_l)/2\right)^2\\
&\quad + m_\beta\left(b(1 - c_l)/2\right)^2 + m_\gamma\left(b(1 + c_t)/2\right)^2,\\
I_\beta &= J_\beta + m_\beta\left(b(1 + c_l)/2\right)^2,\\
I_\gamma &= J_\gamma + m_\gamma\left(b(1 - c_t)/2\right)^2.
\end{aligned}$$

2.2 Aerodynamic Model

The aerodynamic model is based on that given in Theodorsen and Garrick [1942], which considers a wing-flap-tab combination. Using the transformation given in Fig. 3 (see Graham et al. [2011a] for an expanded treatment of these details), and setting a, l, m in (22)-(25) of Theodorsen and Garrick [1942] to zero, we can find the aerodynamic force L and moment M acting on the whole bridge assembly, and the aerodynamic moments M^β and M^γ acting on the leading- and trailing-edge flaps in (1)-(4); see (5)-(9) — the functions $T_i(\cdot)$ and $Y_i(\cdot,\cdot)$ are defined in Theodorsen and Garrick [1942]. Note that M^β is derived using $M^\beta = M_{\beta c} + c_l b L - M$. The heave and pitch corrections mentioned in the caption of Fig. 3 involve replacing h by $h + c_l b\beta$, and replacing α by $\alpha - \beta$, the first and second derivatives of h and α are adjusted similarly in (22)-(25) of Theodorsen and Garrick [1942]. This procedure has been checked in Graham et al. [2011a] against a vortex panel numerical method, which makes the thin aerofoil assumptions, and very close agreement is demonstrated.

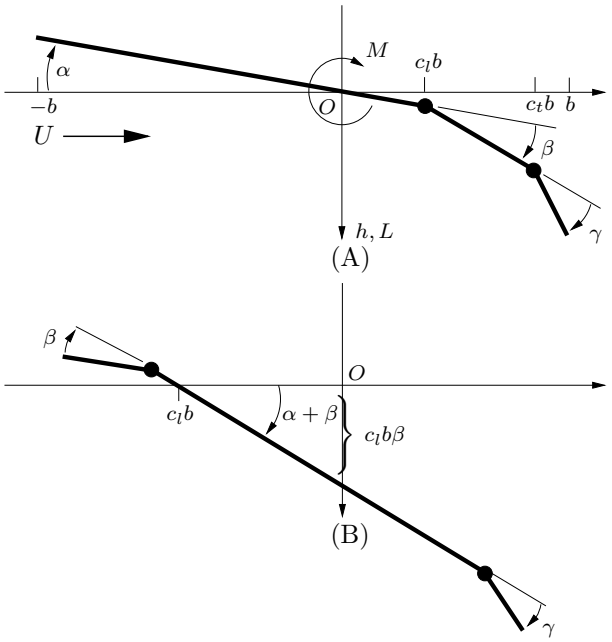

Fig. 3. Transformation of the Theodorsen-Garrick wing-aileron-tab configuration Theodorsen and Garrick [1942] into a bridge deck with controllable leading- and trailing-edge flaps. In (A) the angles of wing pitch, aileron and tab are α, β and γ which are positive clockwise. The wind speed U is positive to the right, the heave h is positive downwards, as is the lift L. The moments are positive clockwise. The wing chord (including flap and tab) is $2b$, and the width of the aileron and tab are specified by c_l and c_t respectively. In (B): The wing-aileron-tab configuration is transformed into the bridge deck with controllable flaps by making c_l negative Graham et al. [2011a]. Pitch and heave corrections must be applied to re-level the bridge i.e., returning its mass center to correct position.

The important Theodorsen function $C(k)$ that appears in (5)-(9) is an irrational function of reduced frequency $k = \omega b/U$ Bisplinghoff et al. [1955]. It is given by

$$C(k) = \frac{J_1(k) - jY_1(k)}{(J_1(k) + Y_0(k)) - j(J_0(k) - Y_1(k))}, \qquad (10)$$

in which $J_0(k)$, $J_1(k)$, $Y_0(k)$ and $Y_1(k)$ are Bessel functions of the first and second kind respectively, and $j = \sqrt{-1}$. To use classical control-theoretic means such as root-locus diagrams, we found an accurate quartic approximation of $C(k)$ in Graham et al. [2011a], whose numerator and denominator coefficients are given in Table 1. Here $\hat{s} = \frac{sb}{U}$

numerator terms	denominator terms
0.99592	1
57.01896 $\hat{s}$	62.30441 $\hat{s}$
623.78848 $\hat{s}^2$	807.78489 $\hat{s}^2$
1895.46328 $\hat{s}^3$	3060.67868 $\hat{s}^3$
1523.24700 $\hat{s}^4$	3033.76379 $\hat{s}^4$

Table 1. Numerator and denominator coefficients of a quartic approximation to the Theodorsen function.

is the reduced Laplace transform variable.

3. FEEDBACK SYSTEM

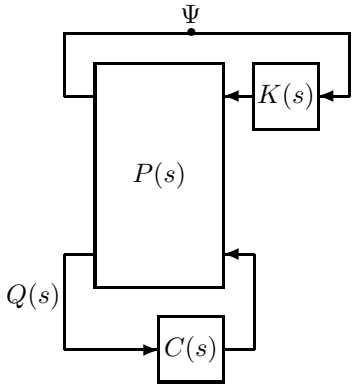

Fig. 4. Block diagram of the aerodynamic control system. The plant P represents the bridge dynamics and non-circulatory fluid mechanic dynamics, $C(s)$ is the Theodorsen circulation function approximation. $Q(s)$ is the lift-producing signal (the relative vertical velocity of the air stream to the bridge deck). $K(s)$ is the controller with feedback signal Ψ. In Fig. 5 the outputs of $K(s)$ (inputs of $P(s)$) are torques acting on the flaps while its inputs Ψ (outputs of $P(s)$) are the vertical velocity of flap pivots.

Fig. 4 shows the bridge control system, which includes the structural and fluid dynamics as well as the control system. $P(s)$ is the uncontrolled open-loop system including the non-circulatory fluid mechanics and the structural dynamics. $C(s)$ is the Theodorsen function approximation which contains the circulatory fluid dynamics.

$$K(s) = \begin{bmatrix} K^\beta(s) & 0 \\ 0 & K^\gamma(s) \end{bmatrix}$$

is the controller which operates the leading- and trailing-edge flaps.

Fig. 5 shows a mechanical feedback control system; h, α, β and γ are the deck's heave, pitch angle, leading- and

$$L = -\rho b^2 \left\{ \pi \ddot{h} + U\pi\dot{\alpha} - (UT_4(c_l) + U\pi)\dot{\beta} - (T_1(c_l)b - \pi c_l b)\ddot{\beta} - UT_4(c_t)\dot{\gamma} - T_1(c_t)b\ddot{\gamma} \right\} - 2\pi\rho UbCQ \tag{5}$$

where

$$Q = \dot{h} + U\alpha + \frac{1}{2}b\dot{\alpha} + \left(\frac{1}{\pi}T_{10}(c_l)U - U\right)\beta + \left(\frac{1}{2\pi}T_{11}(c_l)b + c_l b - \frac{1}{2}b\right)\dot{\beta} + \frac{1}{\pi}T_{10}(c_t)U\gamma + \frac{1}{2\pi}T_{11}(c_t)b\dot{\gamma} \tag{6}$$

$$M = -\rho b^2 \left\{ \frac{1}{2}\pi U b\dot{\alpha} + \frac{1}{8}\pi b^2\ddot{\alpha} + T_{15}(c_l)U^2\beta + \left(T_{16}(c_l)Ub - \frac{1}{2}\pi Ub\right)\dot{\beta} + \left(2T_{13}(c_l)b^2 - \frac{1}{8}\pi b^2\right)\ddot{\beta} \right.$$
$$\left. + T_{15}(c_t)U^2\gamma + T_{16}(c_t)Ub\dot{\gamma} + 2T_{13}(c_t)b^2\ddot{\gamma} \right\} + \pi\rho Ub^2CQ \tag{7}$$

$$M^\beta = \rho b^2 \left\{ (T_1(c_l)b - c_l b\pi)\ddot{h} + \left(\frac{1}{2}\pi Ub - T_{17}(c_l)Ub - c_l bU\pi\right)\dot{\alpha} + \left(\frac{1}{8}\pi b^2 - 2T_{13}(c_l)b^2\right)\ddot{\alpha} \right.$$
$$+ \left(T_{15}(c_l)U^2 - \frac{1}{\pi}T_{18}(c_l)U^2\right)\beta + \left(T_{16}(c_l)Ub - \frac{1}{2}\pi Ub - \frac{1}{\pi}T_{19}(c_l)Ub + T_{17}(c_l)Ub + c_l b(UT_4(c_l) + U\pi)\right)\dot{\beta}$$
$$+ \left(4T_{13}(c_l)b^2 - \frac{1}{8}\pi b^2 + \frac{1}{\pi}T_3(c_l)b^2 + T_1(c_l)c_l b^2 + c_l b(T_1(c_l)b - \pi c_l b)\right)\ddot{\beta} + \left(T_{15}(c_t)U^2 - \frac{1}{\pi}Y_9(c_l, c_t)U^2\right)\gamma$$
$$\left. + \left(T_{16}(c_t)Ub - \frac{1}{\pi}Y_{10}(c_l, c_t)Ub + c_l bUT_4(c_t)\right)\dot{\gamma} + \left(2T_{13}(c_t)b^2 + \frac{1}{\pi}Y_6(c_l, c_t)b^2 + c_l T_1(c_t)b^2\right)\ddot{\gamma} \right\}$$
$$-(\pi + T_{12}(c_l) + 2\pi c_l)\rho Ub^2CQ, \tag{8}$$

$$M^\gamma = -\rho b^2 \left\{ -T_1(c_t)b\ddot{h} + T_{17}(c_t)Ub\dot{\alpha} + 2T_{13}(c_t)b^2\ddot{\alpha} + \frac{1}{\pi}Y_{17}(c_l, c_t)U^2\beta \right.$$
$$+ \left(\frac{1}{\pi}Y_{18}(c_l, c_t)Ub - T_{17}(c_t)Ub\right)\dot{\beta} - \left(\frac{1}{\pi}Y_6(c_l, c_t)b^2 + T_1(c_t)c_l b^2 + 2T_{13}(c_t)b^2\right)\ddot{\beta} + \frac{1}{\pi}T_{18}(c_t)U^2\gamma$$
$$\left. + \frac{1}{\pi}T_{19}(c_t)Ub\dot{\gamma} - \frac{1}{\pi}T_3(c_t)b^2\ddot{\gamma} \right\} - T_{12}(c_t)\rho Ub^2CQ \tag{9}$$

trailing-edge flap angles respectively. M^β and M^γ the aerodynamic moments acting on the leading- and trailing-edge flaps respectively. The control system has two pinions that are mounted on the bridge deck and attached to the flaps. There are also two racks with one ends attached to flaps and the other ends linked to the passive mechanical controllers which are attached to the inertial reference frame and have admittances $Y_l(s)$ and $Y_t(s)$. The inputs and outputs of $Y_l(s)$, $Y_t(s)$ and $K(s)$ of Fig. 4 are the vertical velocity of the flap pivots and torques acting on the flaps respectively. As the deck moves, $Y_l(s)$ and $Y_t(s)$ drive the leading- and trailing-edge flaps through rack-and-pinion connection. A similar controller is suggested in Limebeer et al. [2011] to actuate a trailing-edge flap.

The network through-variable associated with $K^\gamma(s)$ is the force $F_t(s)$, while its across-variable is $\dot{h} + c_t b\dot{\alpha} - r\dot{\gamma}$. Thus

$$F_t(s) = sY_t(s)(h + c_t b\alpha - r\gamma)(s)$$

and so

$$M^\gamma(s) = srY_t(s)(h + c_t b\alpha - r\gamma)(s)$$

giving

$$K^\gamma(s) = rY_t(s).$$

Similarly we derive that

$$M^\beta(s) = srY_l(s)(h + c_l b\alpha - r\beta)(s)$$

and

$$K^\beta(s) = rY_l(s).$$

The control system in Fig. 5 is insensitive of the wind direction if we let $Y_l(s) = Y_t(s)$. We omit the proof here because of page limit, but it will be given in the journal version of this paper.

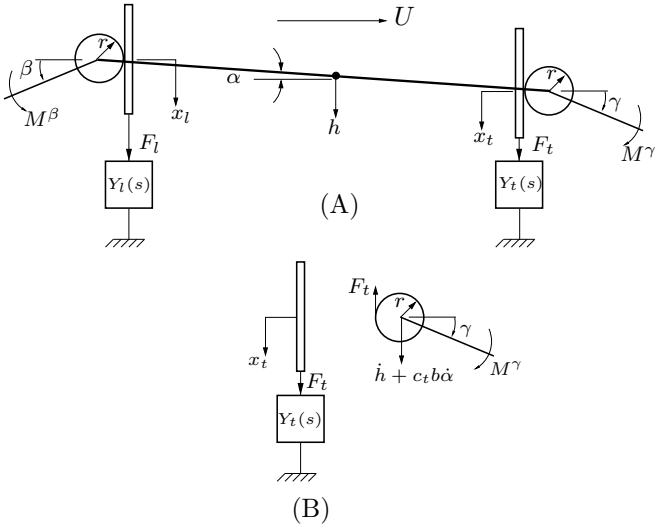

Fig. 5. A prototypical mechanical feedback control system. Figure (A) is a conceptual passive control system. Figure (B) is a free body diagram of the trailing-edge flap system which is used to derive the equations of motion.

4. APPLICATION ON AKASHI KAIKYO BRIDGE

We will use the Akashi-Kaikyo bridge as a working example. This bridge links the city of Kobe (which is on the mainland of Honshu) to Iwaya (which is on Awaji Island) over the Akashi Strait. Akashi Strait often has severe storms — a storm sank two ferries in 1955, which killed 168 people. In 1998 the bridge was open for traffic and has the

longest central span in the world. The parameter values for the bridge Omenzetter et al. [2000b] and example flaps are given in Table 2 in which d_β (d_γ) and ρ_β (ρ_γ) are the average thickness and density respectively of the flap. These parameters will be used in the structure model (1)-(4) and aerodynamic model (5)-(9). The trailing-edge

Parameters	Values
b	$15\,m$
m_d	$33600\,kg$
J_d	$4.97\times10^6\,kg\,m^2$
ω_α	$0.917\,rad/s$
ω_h	$0.427\,rad/s$
ρ	$1.23\,kg/m^3$
$\omega_\beta,\omega_\gamma$	$30\,rad/s$
ρ_β,ρ_γ	$7850\,kg/m^3$
d_β,d_γ	$0.01\,m$

Table 2. Physical parametrs of the Akashi Kaikyo bridge section with controllable flaps

flap's mass per unit span and its moment of inertia around the hinge line are given by

$$m_\gamma = b(1-c_t)\rho_\gamma d_\gamma \quad \text{and} \quad J_\gamma = \rho_\gamma d_\gamma (b(1-c_t))^3/3$$

respectively, similarly for m_β and J_β of the leading-edge flap. The flaps and bridge deck are treated as aerodynamically 'thin'. The flap resonant frequencies ω_β and ω_γ are chosen such that they will not decrease the critical wind speeds for flutter and torsional divergence in the absence of the controllers.

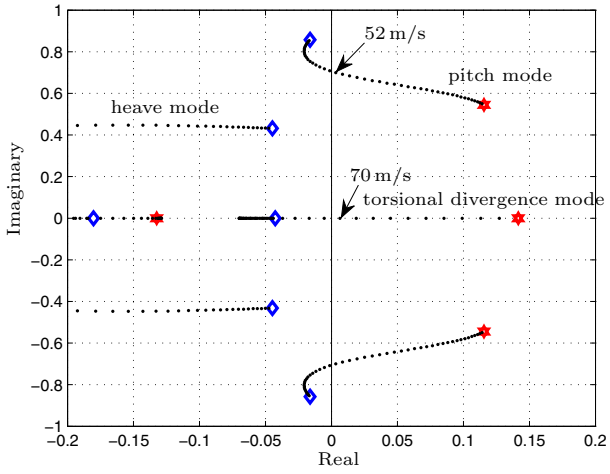

Fig. 6. Root-loci of the uncontrolled bridge section. The wind speed is swept from 30 m/s to 80 m/s, with the low-speed end of the root loci marked with (blue) diamonds and the high-speed ends marked with (red) hexagons. The critical flutter speed is 52 m/s, while the critical torsional divergence speed is approximately 70 m/s. Besides the flutter modes (involving the heave mode and pitch mode) and the torsional divergence mode, there are loci associated with the quartic approximation of the Theodorsen function.

From Fig. 6, the bridge's critical flutter speed and critical torsional divergence speed are approximately 52 m/s and 70 m/s respectively. The design aim is to increase the critical flutter speed to a value just below the divergence speed of 70 m/s by using the mechanical control system in Fig. 5. This control system should have robustness against modelling errors and uncertainty. For this, we seek a mechanical control systems that stabilizes the nominal closed loop and will achieves the following closed-loop mini-max objective:

$$\min_p \left\{ \max_{G_i(s,p)} \| \left(I + G_i(s,p)\right)^{-1} \|_\infty \right\} \quad i = 1,\dots n, \qquad (11)$$

where $G_i(s,p)$ are open-loop multi-variable transfer functions corresponding to wind speeds U_i $i = 1,\dots,n$, which can be obtained by opening the feedback loop at Ψ in Fig. 4. $\|\cdot\|_\infty$ is the infinity norm Green and Limebeer [1995]; s is the Laplace transform variable while p is a parameter set including the parameters of the compensators, the flap chords as well as the pinion radius r. The index (11) corresponds to the closed-loop stability robustness to multiplicative perturbations Green and Limebeer [1995], which is optimized using the MATLAB's sequential quadratic programming algorithm FMINCON The Mathworks Inc. [2000].

We set three constraints for (11) to ensure that the optimization problem is properly posed. The first constraint is system stability for which we constrain the real parts of all the closed-loop eigenvalues to be negative. The second constraint is the passivity of the compensators $Y_l(s)$ and $Y_t(s)$, by imposing a positive-real constraint on the coefficients of the compensators Anderson and Vongpanitlerd [1973]. This constraint allows compensators to be synthesized using passive mechanical components (dampers, springs and inerters) Smith [2002]. The third constraint is the width of flap chord which is set to be positive and less than 2 meters here.

We first assume the compensators were be a first-order passive network of the form:

$$Y(s) = k\frac{s+z_0}{s+p_0}, \qquad (12)$$

in which k, z_0 and p_0 are constrained to be non-negative to ensure passivity. In the optimization process, we consider the wind speeds to be from 4 m/s to 69 m/s in steps of 5 m/s. By the optimization calculation, we get

$$k = 20936.0141,\ z_0 = 1.2639,\ p_0 = 0.2687, r = 0.4868,$$

with optimal flap chords of 1.5579 m. In this case the index given in (11) equals to 1.4937. Apparently this is a lag compensator. A physical realization of $Y(s)$ is given in Fig. 7. It is easy to check that

$$D_1 = k, \quad K_1 = k(z_0 - p_0), \quad D_2 = k(\frac{z_0}{p_0} - 1).$$

Fig. 8 shows the associated closed-loop root loci, where it is also clear that the closed-loop system is stable with the critical flutter speed increased to approximately 70 m/s.

We also conducted a further design study using second-order passive compensators, but the improvement of robust performance over the first-order compensator above was marginal.

5. CONCLUSIONS

In this paper we greatly improved the critical flutter speed of a suspended-span bridge section using controlled flaps

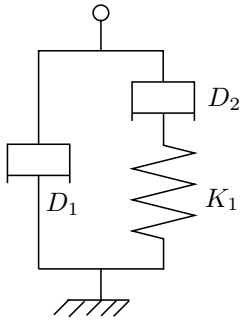

Fig. 7. Realization of the first-order mechanical lag compensators shown in Fig. 5 as $Y_l(s)$ and $Y_t(s)$ and given in equation (12).

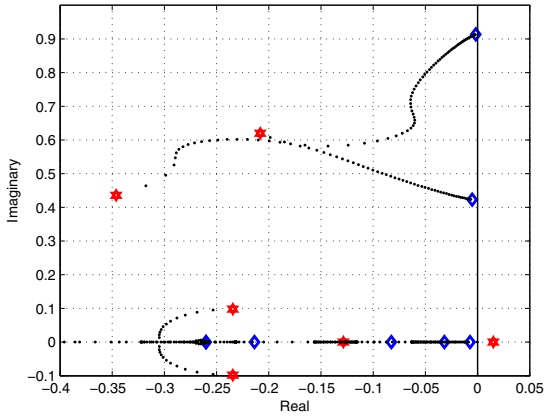

Fig. 8. Closed-loop root-locus for the symmetrically controlled bridge deck; the wind speed is swept from 5 m/s to 70 m/s, with the low wind speed ends of each locus marked with blue diamonds and high wind speed ends marked with the red hexagons. In addition to the dynamics given Fig. 6, the root loci given here include the dynamics of the flaps and the control system.

operated by a mechanical control system with good robustness. The control system is independent to wind speed. The buffeting suppression problem will be treated in the journal version of this paper. This paper makes the assumption that the grounded sides of the compensation networks $Y_l(s)$ and $Y_t(s)$ are connected to stationary points in an inertial reference frame. However, in some cases, it might be necessary to make use of compensation network anchor points that are attached to a large, but compliant structure. The effect of flexible mounting arrangements for a trailing-edge mechanical controller have been considered in Limebeer et al. [2011] and these adjustments may be applied here too.

REFERENCES

B. D. O. Anderson and S. Vongpanitlerd. *Network analysis and synthesis: a modern systems theory approach*. Englewood Cliffs, N.J., Prentice-Hall, 1973.

M. A. Astiz. Flutter stability of very long span bridges. *Journal of Bridge Engineering*, 3(3):132–139, 1998.

K. Y. Billah and R. H. Scanlan. Resonance, tacoma narrows bridge failure, and undergraduate physics textbooks. *American Journal of Physics*, 59(2):118–124, 1991.

R. L. Bisplinghoff, H. Ashley, and R. L. Halfman. *Aeroelasticity*. Addison-Wesley, 1955.

D. Cobo del Arco and A. C. Aparicio. Improving suspension bridge wind stability with aerodynamic appendages. *Journal of Structural Engineering*, 125(12): 1367–1375, 1999.

S. Evangelou, D. J. N. Limebeer, R. S. Sharp, and M. C. Smith. Steering compensators for high-performance motorcycles. *ASME J. Applied Mechanics*, 74(5):332–346, 2007.

J. M. R. Graham, D. J. N. Limebeer, and X. Zhao. Aeroelastic control of long-span suspension bridges. *ASME J. Applied Mechanics*, 78(4):041018.1 – 041018.12, 2011a.

J. M. R. Graham, David J. N. Limebeer, and X. Zhao. Aeroelastic moldelling of long-span suspension bridges. In *Proc. of the 18th IFAC World Congress*, pages 9212 – 9217, Milan, 28 August to 2 September 2011b.

M. Green and D. J. N. Limebeer. *Linear Robust Control*. Prentice Hall, Englewood Cliffs, New Jersey, 1995.

H. I. Hansen and P. Thoft-Christensen. Active flap control of long suspension bridges. *Journal of Structural Control*, 8(1):33–82, 2001.

D. J. N. Limebeer, J. M. R. Graham, and X. Zhao. Buffet suppression in long-span suspension bridges. *Annual Reviews in Control*, 35:235–246, 2011.

P. Omenzetter, K. Wilde, and Y. Fujino. Suppression of wind-induced instabilities of a long span bridge by a passive deck-flaps control system part I: Formulation. *Journal of Wind Engineering*, 87:61–79, 2000a.

P. Omenzetter, K. Wilde, and Y. Fujino. Suppression of wind-induced instabilities of a long span bridge by a passive deck-flaps control system part II: Numerical simulations. *Journal of Wind Engineering*, 87:81–91, 2000b.

M. C. Smith. Synthesis of mechanical networks: The inerter. *IEEE Trans. Automatic Control*, 47(10):1648–1662, 2002.

The Mathworks Inc. *MATLAB 6 Reference Manual*, 2000. URL `http://www.mathworks.com`.

T. Theodorsen and I. E. Garrick. Nonstationary flow about a wing-aileron-tab combination including aerodynamic balance. *NACA Report, TR-736*, 1942.

K. Wilde and Y. Fujino. Variable-gain control applied to aerodynamic control of bridge deck flutter. pages 682–687. Proceedings of 35th Conference on Decision and Control, Kobe, Japan, 1996.